NAVIGATION SYSTEM FOR LANDING A SWARM OF AUTONOMOUS DRONES ON A MOVABLE SURFACE

Anam Tahir[1, a], Jari Böling[2, b], Mohammad-Hashem Haghbayan[1, c], and Juha Plosila[1, d]
[1]Autonomous Systems Laboratory, Department of Future Technologies
[2]Laboratory of Process and Systems Engineering
[1]University of Turku, [2]Åbo Akademi University
[1,2]Turku, Finland
Email: [a]anam.tahir@utu.fi, [b]jari.boling@abo.fi, [c]mohhag@utu.fi, [d]juha.plosila@utu.fi

KEYWORDS

Unmanned Aerial Vehicles; Distributed Control; Leader–Follower Hierarchy; Soft Landing

ABSTRACT

The development of a navigation system for the landing of a swarm of drones on a movable surface is one of the major challenges in building a fully autonomous platform. Hence, the purpose of this study is to investigate the behaviour of a swarm of ten drones under the mission of soft landing on a movable surface that has a linear speed with the effect of oscillations. This swarm, arranged in a leader–follower hierarchical manner, has distributed control units based on Linear Quadratic Regulator control with integral action technique. Furthermore, to prevent drones from landing arbitrarily, the leader drone takes the feedback of translational coordinates from the movable surface and adjusts its position accordingly. Hence, each follower tracks the leader's trail with offsets, taking collision avoidance into account. The design parameters of controllers are mapped in a way that the simulations demonstrate the feasibility and great potential of the proposed method.

INTRODUCTION

Unmanned Aerial Vehicles (UAVs), or drones, are increasingly getting attention in the aviation and maritime industries with the evolution of drone technology for both recreational and military grounds [1, 2]. These have innovative impacts in the areas of data collection for inspection purposes and are capable of carrying out tasks in a variety of situational operations. They can shape the future with potential benefits in the fields such as security and surveillance, remote sensing, search and rescue, elimination of human error, and autonomous deliveries and shipping [3–6]. For example, in 2017, the European Maritime Safety Agency (EMSA) issued a contract to Martek, valued at €67M for the usage of drones in European waters to provide assistance with border control activities, pollution monitoring, search and rescue tasks, and detection of illegal trafficking (drugs and people) and fishing [7, 8].

The landing mechanism of UAVs is one of the challenging problems. An extensive survey based on vision-based autonomous landing methods is elaborated in [9]. Based on the setup of the vision sensors, these methods are divided into two main categories, i.e., onboard vision landing systems and on-ground vision systems. In [10], a detailed review on control based landing techniques (such as from basic nonlinear to intelligent, hybrid and robust control) along with GPS and vision-based landing schemes is presented. A wide literature is available related to vision-based autonomous landing of UAVs [11–17]. For example, in [18], a vision-based net recovery landing system is proposed for a fixed-wing UAV that does not require a runway. Likewise in [19], the landing of a quadrotor on a moving platform is addressed. In [20], a real-time vision-based landing algorithm for an autonomous helicopter is implemented. An on-board behaviour-based controller is used that is subdivided into hover, velocity, and sonar sub-behaviours. Hovering control of the helicopter is implemented using proportional control, whereas velocity and sonar controllers are implemented with proportional-integral control design. In [21], a nonlinear proportional-integral type controller is proposed for vertical take-off and landing of a quadcopter. It exploits the vertical optical flow to facilitate hover and land on a movable platform. In [22], to control a quadcopter's vertical take-off and landing on a moving platform, the image-based visual servoing integrated with the adaptive sliding mode controller is validated. However, this approach requires the landing site to be predetermined and therefore, it is not suitable for operations in unknown terrain.

Due to the rising importance and research effort put into autonomous vehicles and robots, there is broad research on vision-based methods integrated with/without control techniques for landing missions. Hence, this paper focuses on the control design for landing a swarm of drones on a movable surface, and the vision-based approaches are of no interest in this work.

Communications of the ECMS, Volume 34, Issue 1,
Proceedings, ©ECMS Mike Steglich, Christian Mueller,
Gaby Neumann, Mathias Walther (Editors)
ISBN: 978-3-937436-68-5/978-3-937436-69-2(CD) ISSN 2522-2414

Landing safely, i.e., soft landing, is the key to successful exploration of the assigned missions; in electromechanical systems, the mitigation of the connected effects of collision relies on the conversion of kinetic energy into heat or potential energy. An effective landing-system design should minimize the acceleration acting on the payload. In other words, the major challenges in autonomous landing are; (a) accurate placements as much as possible on the landing platform, and (b) the trajectory following in the presence of disturbances and uncertainties. Portions of this work have been reported in the previous work [23]. However, for present paper, there are additional contributions to face these challenges. This paper addresses the problem based on system modelling and testing of a swarm in a leader–follower hierarchical formation, consisting of ten drones, aiming at executing missions of soft landing on an oscillating surface that can be a vessel or any surface having oscillations. The distributed control units of each quadcopter in the swarm are designed using an Linear Quadratic Regulator (LQR) with integral action technique that can handle a multivariable system.

This paper comprises of 6 sections. Section 1, in addition to introducing the topic, also dwells upon the significance of the study as well as the works already carried out in this particular domain. Section 2 discusses the elements of a swarm formation while Section 3 elaborates the composition of swarm formation of UAVs. Section 4 describes the proposed control design for soft landing, whereas Section 5 builds upon the evaluation of the landing missions. Lastly, Section 6 presents the concluding remarks.

COMPONENTS OF A FORMATION

One of the most vital challenges in multi-agent systems is the formation control. It is defined as an organisation of a group of agents to maintain a formation with a certain shape [6]. Three main components are considered to solve any formation control problem, i.e., system architecture, its modelling, and strategies of formation control [24].

System Architecture

The system architecture delivers the infrastructure upon which formation control is implemented such as:

- Heterogeneity vs. homogeneity: Heterogeneous teams consist of either different apparatus or software, whereas homogeneous teams comprise of similar modules of hardware or software.
- Communication structures: The communication structures in the swarm can be categorised w.r.t. range, topology, and bandwidth.
- Centralization vs. decentralization: In the centralized controlling approach, a single controller possesses all the information required to get the desired control objectives, whereas each agent has its own local control mechanism and is completely autonomous in the decision process of decentralized control. Hybrid centralized/decentralized architectures, in turn, use central planners to provide high-level control over autonomous robots.

System Dynamics

The dynamics of each drone in the swarm is based on the model of a quadcopter, i.e., a drone that has four propellers and ℓ is a length of the fixed pitch to mechanically movable blades, as shown in Fig. 1.

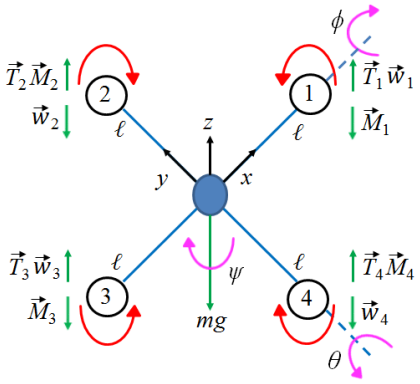

Fig. 1: Kinematics of the quadcopter

The gravity g and the thrust T_i, $i \in \{1, 2, 3, 4\}$, of the propellers are the main forces acting on the quadcopter. In this model, the inertial reference is the earth shown as (x, y, z) that is the origin of the reference frame. The drone is assumed to be a rigid body that has the constant mass symmetrically distributed with respect to the planes (x, y), (y, z), and (x, z). The orientation of a quadcopter reference frame (x, y, z) with respect to an inertial frame $(x, y, z)_0$ can be expressed mathematically in a state variable form [25], where translational and angular accelerations are given by

$$\begin{aligned} \dot{v}_x &= -v_z w_y + v_y w_z - g\sin\theta \\ \dot{v}_y &= -v_x w_z + v_z w_x + g\cos\theta\sin\phi \\ \dot{v}_z &= -v_y w_x + v_x w_y + g\cos\theta\cos\phi - \frac{T}{m} \end{aligned} \tag{1}$$

and

$$\begin{aligned} \dot{w}_x &= \frac{1}{J_x}(-w_y w_z(J_z - J_y) + M_x - \frac{k_{wT}}{k_{MT}} J_{mp} M_z w_y) \\ \dot{w}_y &= \frac{1}{J_y}(-w_x w_z(J_x - J_z) + M_y - \frac{k_{wT}}{k_{MT}} J_{mp} M_z w_x) \\ \dot{w}_z &= \frac{M_z}{J_z} \end{aligned} \tag{2}$$

respectively. The thrust produced by each propeller T_i is translated into a total thrust T, and the reactive torque M_i, $i \in \{x, y, z\}$, is affecting the rotations along the corresponding axis. J_i, $i \in \{x, y, z\}$, is known as the moment of inertia along the corresponding axis, and J_{mp} is the moment of inertia of a motor with a propeller. The velocities corresponding to Equations (1) and (2) are

$$
\begin{aligned}
\dot{x} &= v_x \cos\psi \cos\theta + v_y(-\sin\psi \cos\phi + \cos\psi \sin\theta \\
&\quad \sin\phi) + v_z(\sin\psi \sin\phi + \cos\psi \sin\theta \cos\phi) \\
\dot{y} &= v_x \sin\psi \cos\theta + v_y(\cos\psi \cos\phi + \sin\psi \sin\theta \\
&\quad \sin\phi) + v_z(-\cos\psi \sin\phi + \sin\psi \sin\theta \cos\phi) \\
\dot{z} &= v_x \sin\theta - v_y \cos\theta \sin\phi - v_z \cos\theta \cos\phi
\end{aligned} \tag{3}
$$

and

$$
\begin{aligned}
\dot{\theta} &= w_y \cos\phi - w_z \sin\phi \\
\dot{\phi} &= w_x + w_y \sin\phi \tan\theta + w_z \cos\phi \tan\theta \\
\dot{\psi} &= w_y \frac{\sin\phi}{\cos\theta} + w_z \frac{\cos\phi}{\cos\theta}
\end{aligned} \tag{4}
$$

respectively. The Equations (1)–(4) represent the complete nonlinear model of a quadcopter, composed of 12 states, 4 inputs, and 12 outputs. More precisely,

$$
\mathbf{x} = \begin{bmatrix} v_x & v_y & v_z & w_x & w_y & w_z & \theta & \phi & \psi & x & y & z \end{bmatrix}^{\mathrm{T}} \tag{5}
$$

is the state or system vector,

$$
\mathbf{u} = \begin{bmatrix} T & M_x & M_y & M_z \end{bmatrix}^{\mathrm{T}} \tag{6}
$$

is the input or control vector,

$$
\mathbf{y} = \mathbf{x} \tag{7}
$$

is the output (measured) vector. Furthermore, the performance output

$$
\mathbf{y_p} = \begin{bmatrix} x & y & z \end{bmatrix}^{\mathrm{T}} \tag{8}
$$

is defined for future use.

Using standard linearization, that is cutting off a Taylor series expansion after the first derivative, the nonlinear dynamic equations can be converted into linear state-space equations. This yields,

$$
\begin{aligned}
\dot{\mathbf{x}} &= \begin{bmatrix} -g\theta & g\phi & -\frac{T}{m} & \frac{M_x}{J_x} & \frac{M_y}{J_y} & \frac{M_z}{J_z} & w_y & w_x & w_z & v_x & v_y & -v_z \end{bmatrix}^{\mathrm{T}} \\
\mathbf{y} &= \mathbf{x}
\end{aligned} \tag{9}
$$

that can further written into the standard state space form

$$
\begin{aligned}
\dot{\mathbf{x}} &= A\mathbf{x} + B\mathbf{u} \\
\mathbf{y} &= C\mathbf{x} + D\mathbf{u}
\end{aligned} \tag{10}
$$

where A, B, C, and D are known as the state or system matrix, input or control matrix, output (measured) matrix, and feedthrough matrix respectively. Correspondingly, $\mathbf{x}$, $\mathbf{u}$, and $\mathbf{y}$ are known as the state or system vector, input or control vector, and output (measured) vector as in Equations (5)–(7). The system parameters are taken from [25] and illustrated in Table I. The linear model in Equation (10) is used to examine the landing stability and controllability of the system as well as to design an LQR with integral control. The system has twelve eigenvalues at the origin, and all twelve states are controllable.

TABLE I: System parameters

Symbol	Quantity	Value
g	gravitational force	9.81 m/s^2
ℓ	length of the fixed pitch to mechanically movable blades	0.2 m
m	mass of quadcopter	0.8 kg
J_{mp}	moment of inertia of motor with propeller	≈ 0
J_x, J_y	moment of inertia w.r.t. axis x, y	1.8×10^{-3} kgm^2
J_x	moment of inertia w.r.t. axis z	1.5×10^{-3} kgm^2
k_{MT}	ratio of the reactive moment and thrust	0.1 m

Formation Control Schemes

A formation control scheme defines how a group of robots can be controlled to form and to maintain the desired formation. To control the formation of a drone swarm, the recent studies generally classify the different strategies into following main categories.

- Leader–follower [26–28]: The leader seeks for some group objectives, while the followers track the leader's coordinates with prescribed offsets.
- Virtual structure [29–31]: A virtual moving structure reflects the complete formation as a rigid body such that the control design for a single agent is derived by defining the virtual structure. It then translates the movement of the virtual structure into the desired movement of each agent. Furthermore, as an actual leader is not needed, each virtual vacant pose can be filled by any agent.
- Behaviour-based [32–34]: each agent is assigned to the process of actuation that is defined as several desired behaviours. In each agent, to form the desired shape of the swarm, the overall control is derived by allocating different weights to behaviours.

The formation control schemes can be further categorised into position-, displacement-, distance-, and angle-based in terms of the requirement on the sensing capability and the interaction topology [35]. In position-based control, each agent is able to sense its own position in the formation that is defined by the desired positions of the different agents with respect to a global coordinate system. In contrast to this, in displacement-based control, each agent is assumed to sense its own as well as its neighbouring agents' position in the formation that is defined by the desired displacements between pairs of agents with respect to

the global coordinate system. Then again, in distance-based control, the formation is defined by the desired inter-agent distances that are actively controlled. Each agent in the formation is expected to sense relative positions of their neighbouring agents with respect to their own local coordinate systems. Likewise, the actively controlled variable is the bearing between neighbours in angle-based control, rather than the distance to each of the neighbours.

COMPOSITION OF SWARM OF UAVS

Consider a hierarchical formation that has four levels using ten quadcopters, as illustrated in Fig. 2. This formation is based on a tightly coupled leader–follower flying mechanism in which the leader is directly communicating with its followers by providing its position references that are passed on to the followers [6, 36].

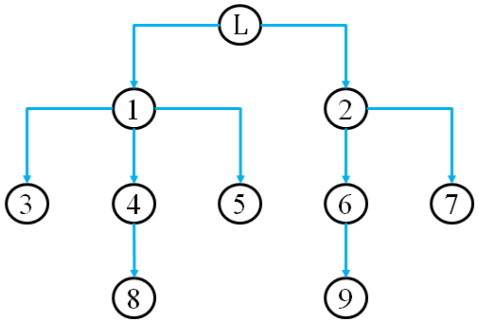

Fig. 2: Organization of the considered swarm of drones

In Fig. 2, the swarm is responsible for tracking the desired trajectories as well as for hovering at desired positions for given time intervals. The straight arrows show the direction in which coordinate variables are shared. The leader's trajectory is independent and defines the formation's trajectory. The trajectory of each follower is defined based on the orientation and actions of its respective leader. In terms of movement, each follower is dependent on its respective leader's movement using a safe distance strategy that is denoted by $d_{\alpha,\beta}$, where $\alpha, \beta \in \{\mathrm{L}, 1\text{–}9\}$. Each follower is responsible for efficiently tracking the respective leader's trajectory, maintaining the distance between two respective entities.

To address the research questions, consider a control system that is liable for fine-tuning the movement of each drone in a swarm while maintaining the desired safe travel distance. Each drone is based on the similar system dynamics, which is illustrated in Section 2. In Fig. 3, a simple mechanism of feedback control system is presented in which output is controlled using its measurement as a feedback signal. This feedback signal is compared with a reference signal to generate an error signal which is filtered by a controller to produce the system's control input.

PROPOSED CONTROL DESIGN FOR SOFT LANDING

In a simple example illustrated in Fig. 4, the swarm of drones aims to land on a vessel (or any type of movable surface) that has continuous speed with oscillations. It is assumed that the data is available through communication link on-board drones and vessel.

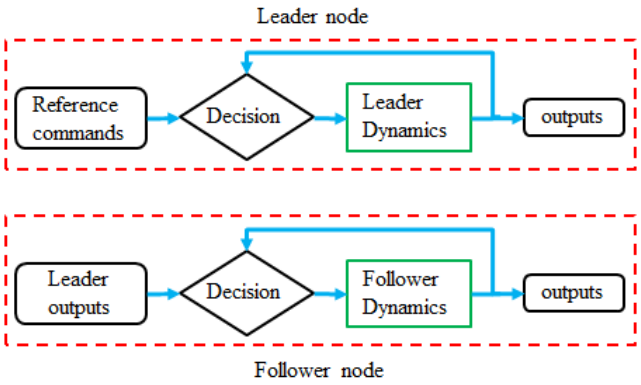

Fig. 3: Transmission topology in swarm formation

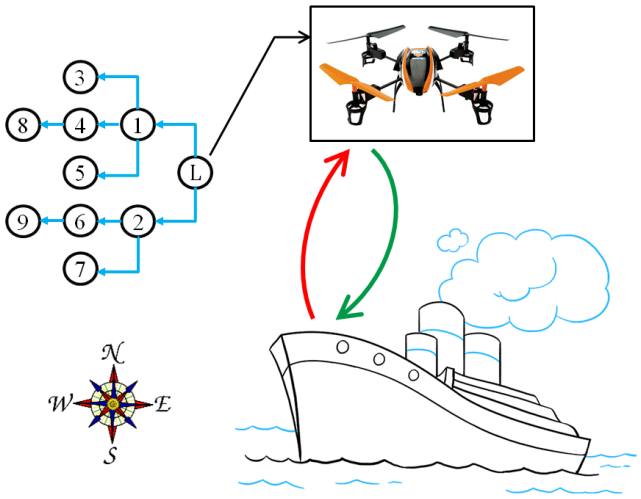

Fig. 4: Arrival of the swarm of drones for landing

In Fig. 4, the reference commands of a moving vessel are continuously sent to the leader drone as a feedback (red arrow line), outlining a tracking phenomenon. The local control unit of the leader then computes the values under its vicinity and generates the force in order to stabilize its landing movement (green arrow line). This process continuous until the desired goal is achieved. Since, the designed formation is based on a leader–follower tightly coupled approach therefore, all the followers track their corresponding leaders, which can minimize the overall computation time of path planning, indicating the fast decision making within the swarm. A filter block (see Appendix) is included in the altitude of the leader drone to slow down its speed on a close arrival by avoiding sudden hit on the surface.

For the controlled movement of each quadcopter in the swarm, the initial step is to construct a balanced drone in the presence of uncertainties and external disturbances with an adaptive computing platform. For this study, a standard LQR with integral action technique has been adapted [36]. Based on the linear model in Equation (10), LQR is a way of finding an optimal

full state feedback controller for each quadcopter. Fig. 5 shows the decision-making process of a drone that is split into two feedback loops, i.e., inner and outer loops. The inner loop is the full state feedback system and the outer loop is responsible for the x, y, and z positions, generating the thrust T and the torques M_i.

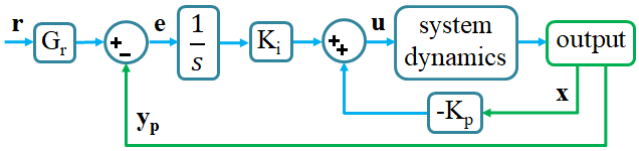

Fig. 5: Block diagram of the control design

The control input $\mathbf{u}$ minimizes the quadratic cost function

$$J(\mathbf{u}) = \int_0^\infty (\dot{\mathbf{x}}_\mathbf{a}^\mathrm{T}\ Q\ \dot{\mathbf{x}}_\mathbf{a} + \dot{\mathbf{u}}^\mathrm{T}\ R\ \dot{\mathbf{u}})dt \qquad (11)$$

where Q and R are known as the weight matrices (see Appendix), and $\mathbf{u}$ is given in Equation (6). The Q matrix is a positive semi-definite that defines the weights for the states, whereas the R matrix is a positive definite that indicates the weights of the control inputs. The controller can be tuned by changing the entries in the Q and R matrices to get the desired response. LQR method returns the solution S of the associated Riccati equation

$$(A)^\mathrm{T}S + SA - SBR^{-1}(B)^\mathrm{T}S + Q = 0 \qquad (12)$$

for $S = S^\mathrm{T} > 0$. The optimal gain matrix K is derived from S as $K = R^{-1}(B)^\mathrm{T}S$. The four control inputs are generated for thrust T, M_x (along x-axis i.e., roll ϕ), M_y (along y-axis i.e., pitch θ), and M_z (along z-axis i.e., yaw ψ) using state feedback law,

$$\mathbf{u} = \frac{K_i}{s}\mathbf{e} - K_p\mathbf{x}, \qquad (13)$$

where $\mathbf{e} = r - y_p$, $\mathbf{r} = [x_r \quad y_r \quad z_r]^\mathrm{T}$, $\mathbf{y_p}$ is given in Equation (8), K_i is the integral gain, and K_p is the state feedback gain.

RESULTS

The landing of the swarm of drones on a movable surface (can be defined as a vessel) that has continuous speed with oscillations, which is moving from south-west to north-east, is considered with a smallest margin of error. The simplest model of a movable surface V is defined as a ramp function with a slope of $0.5t$. The oscillations of a movable surface are defined as sine wave with amplitude of 1m, and frequency of 0.1rad/sec. Since the swarm is arranged in a tightly coupled leader–follower hierarchical formation, the reference signal of the leader drone is available to its immediate follower(s). Thus, the followers track the output of the leader with set distance. The initial time $t = 0$s while the landing occurs at time $t = 15$s, are set in the references of the leader drone. The reference positions of the leader drone are $x = y = 2$, and $z = 10 \longrightarrow 0$ with step time $t = 15$s. The initial launching position x of each drone is set to 7m away from its respective neighbouring node(s), and the further data for simulation is shown in Table II. Simulations in Simulink® MATLAB are used for the evaluation of the proposed method. In all simulations, the sampling time t_s of 0.01s is used for all the figures.

TABLE II: Initial positions (m) and offsets (m) of drones used in simulation

Drones	Symbol	Initial Position $(x, y, z)^*$	Offset $(x, y, z)^*$
Leader	L	$(0, 0, 10)$	–
Follower 1	f1	$(7, 0, 10)$	$(9, 0, 0)$
Follower 2	f2	$(-7, 0, 10)$	$(-5, 0, 0)$
Follower 3	f3	$(14, 0, 10)$	$(9, 0, 0)$
Follower 4	f4	$(21, 0, 10)$	$(16, 0, 0)$
Follower 5	f5	$(28, 0, 10)$	$(23, 0, 0)$
Follower 6	f6	$(-14, 0, 10)$	$(-5, 0, 0)$
Follower 7	f7	$(-21, 0, 10)$	$(-12, 0, 0)$
Follower 8	f8	$(35, 0, 10)$	$(16, 0, 0)$
Follower 9	f9	$(-28, 0, 10)$	$(-12, 0, 0)$

The landing mechanism on a movable surface is shown in Fig. 6(a) and (b). The orientation of the surface is available as a feedback at the leader drone that resulted in accurate landing with negligible errors. Hence, each follower track the reference commands that are defined by its respective leader and the pre-specified formation. To avoid collisions in the swarm, there is a gap of 7m in x positions for all the drones with their neighbouring peer(s). Therefore, it is evident that the landing of all the drones is occurred in a straight line with different x positions. Furthermore, the total kinetic energy, KE, produced by the swarm due to its motion versus the total stored potential energy, PE is described in Fig. 6(c). Total energy possessed and held in the swarm are calculated as $KE = 0.5mv^2$ and $PE = mgh$ respectively. These energies relate how much work is conserved in the process of the swarm movement.

The trajectory errors, $\{e_x, e_y, e_z\}$, between the orientation of the movable surface V and the drones are illustrated in Fig. 7(a), (b), and (c). The trajectory error e_z is sometimes positive in Fig. 7(c) because z position is different depending on y position, and the drones land at different positions and/or time instances.

CONCLUSION

This paper addressed one of the interesting challenges in employment of swarming drones, namely landing softly/safely on a movable surface. More specifically, a setup is considered where a swarm of ten drones in a hierarchical leader–follower formation aims at land-

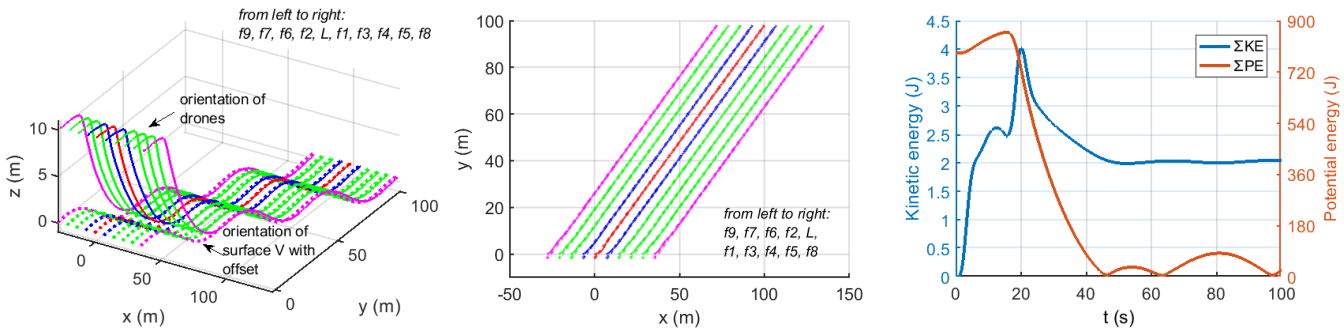

(a) 3D view (b) top view (c) Sum of kinetic vs. potential energies, the drones are moving with the ship after landing

Fig. 6: Landing placements of swarming drones

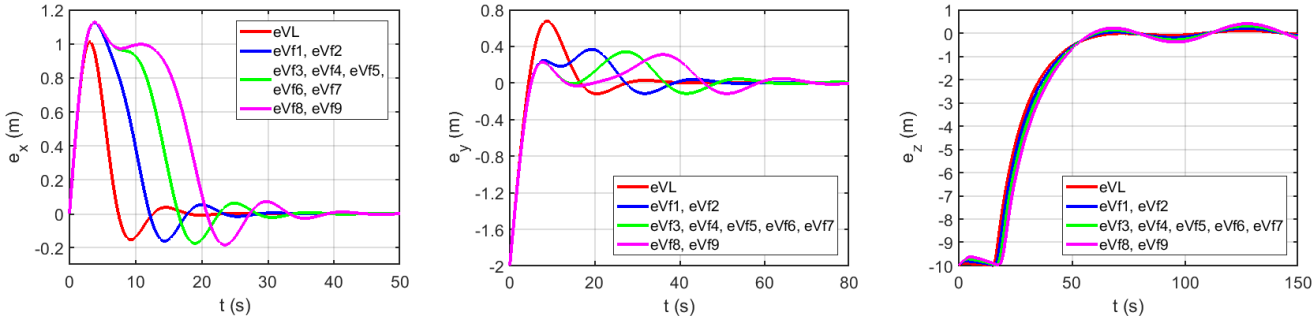

(a) (b) (c)

Fig. 7: Trajectory errors between movable surface and corresponding drone

ing on a moving vessel that has a linear speed under the effect of oscillations. In the proposed distributed control system design, each drone in the swarm has a local controller based on an LQR with integral action technique that is an optimal control method providing the smallest possible error to its input. To avoid any collisions among drones in the swarm, a safe travel distance strategy using offsets is employed in the overall system. In the considered scenario, each drone is already at a specific altitude and from there it lands. The swarm is composed of tightly coupled agents, where each drone in the swarm is directly communicating, using shared coordinate variables, with its immediate associate. Therefore, the leader of the swarm is responsible for the execution of the path planning algorithm. It takes the translational measurements of the movable surface as a feedback in order to generate the landing coordinates. It is evident from the simulation results that the proposed system guarantees the convergence of the desired landing missions on the movable surface while minimizing the possibilities for landing errors. The other key advantages of the proposed method are its robustness and scalability. Furthermore, It is understandable from the graphs that the control strategy permits the intuitive execution of an extensive variety of the swarm behaviours.

APPENDIX

$$Q = \mathrm{diag}\left(\begin{bmatrix} 0.0885, 4.6064e-04, 6000, 1080, 1080, \\ 1080, 180, 180, 180, 0.0147, 7.6773e-05, \\ 1000, 0.4423, 0.0023, 30000 \end{bmatrix} \right)$$

$R = I_4$

Filter block $G_r = \{G_{x_r}, G_{y_r}, G_{z_r}\}$. For the leader drone, $G_{x_r} = G_{y_r} = 1$, and G_{z_r} = state-space model in which $A = -1/12$, $B = 1/12$, $C = 1$, $D = 0$, and initial conditions = 10. For all the other drones, $G_r = \{G_{x_r}, G_{y_r}, G_{z_r}\} = \{1, 1, 1\}$

ACKNOWLEDGEMENTS

This work has been supported in part by the Academy of Finland, project no. 314048.

REFERENCES

[1] G. Collins, D. Twining, and J. Wells, "Using vessel-based drones to aid commercial fishing operations," in *OCEANS 2017 - Aberdeen*, 2017, pp. 1–5.

[2] H. H. Seck. This unmanned rolls royce ship concept could launch drone choppers.

[3] J. Karpowicz. 4 ways drones are being used in maritime and offshore services.

[4] J. Hines. The use of drones in shipping and cover implications.

[5] M. H. Frederiksen and M. P. Knudsen, "Drones for offshore and maritime missions: Opportunities and barriers," in *Denmark: Centre for Integrative Innovation Management*, 2018.

[6] A. Tahir, J. Böling, M.-H. Haghbayan, H. T. Toivonen, and J. Plosila, "Swarms of unmanned aerial vehicles – a survey," *Journal of Industrial Information Integration*, vol. 16 (100106), 2019.

[7] Martek marine named on world's biggest ever €67m maritime drone contract - martek aviation. [Online]. Available: https://www.martekuas.com/martek-marine-awarded-place-remotely-piloted-aircraft-systems-framework-contract-european-maritime-safety-agency/

[8] Drones in the deep: new applications for maritime uavs. [Online]. Available: https://www.ship-technology.com/features/drones-deep-new-applications-maritime-uavs/

[9] W. Kong, D. Zhou, D. Zhang, and J. Zhang, "Vision-based autonomous landing system for unmanned aerial vehicle: A survey," in *2014 International Conference on Multisensor Fusion and Information Integration for Intelligent Systems (MFI)*, 2014, pp. 1–8.

[10] A. Gautam, P. B. Sujit, and S. Saripalli, "A survey of autonomous landing techniques for uavs," in *2014 International Conference on Unmanned Aircraft Systems (ICUAS)*, 2014, pp. 1210–1218.

[11] O. Araar, N. Aouf, and I. Vitanov, "Vision based autonomous landing of multirotor uav on moving platform," *Journal of Intelligent Robotic Systems*, vol. 85, no. 2, p. 369–384, 2017.

[12] M. Meingast, C. Geyer, and S. Sastry, "Vision based terrain recovery for landing unmanned aerial vehicles," in *2004 43rd IEEE Conference on Decision and Control (CDC) (IEEE Cat. No.04CH37601)*, vol. 2, 2004, pp. 1670–1675.

[13] S. Huh and D. H. Shim, "A vision-based automatic landing method for fixed-wing uavs," *Journal of Intelligent and Robotic Systems*, vol. 57, p. 217–231, 2010.

[14] G. Xu, X. Chen, B. Wang, K. Li, J. Wang, and X. Wei, "A search strategy of uav's automatic landing on ship in all weathe," in *2011 International Conference on Electrical and Control Engineering*, 2011, pp. 2857–2860.

[15] J. Park, Y. Kim, and S. Kim, "Landing site searching and selection algorithm development using vision system and its application to quadrotor," *IEEE Transactions on Control Systems Technology*, vol. 23, no. 2, pp. 488–503, 2015.

[16] T. K. Venugopalan, T. Taher, and G. Barbastathis, "Autonomous landing of an unmanned aerial vehicle on an autonomous marine vehicle," in *2012 Oceans*, 2012, pp. 1–9.

[17] T. Templeton, D. H. Shim, C. Geyer, and S. S. Sastry, "Autonomous vision-based landing and terrain mapping using an mpc-controlled unmanned rotorcraft," in *Proceedings 2007 IEEE International Conference on Robotics and Automation*, 2007, pp. 1349–1356.

[18] H. J. Kim, M. Kim, H. Lim, C. Park, S. Yoon, D. Lee, H. Choi, G. Oh, J. Park, and Y. Kim, "Fully autonomous vision-based net-recovery landing system for a fixed-wing uav," *IEEE/ASME Transactions on Mechatronics*, vol. 18, no. 4, pp. 1320–1333, 2013.

[19] P. Serra, R. Cunha, T. Hamel, D. Cabecinhas, and C. Silvestre, "Landing of a quadrotor on a moving target using dynamic image-based visual servo control," *IEEE Transactions on Robotics*, vol. 32, no. 6, pp. 1524–1535, 2016.

[20] S. Saripalli, J. F. Montgomery, and G. S. Sukhatme, "Vision-based autonomous landing of an unmanned aerial vehicle," in *Proceedings 2002 IEEE International Conference on Robotics and Automation (Cat. No.02CH37292)*, vol. 3, 2002, pp. 2799–2804.

[21] B. Hérissé, T. Hamel, R. Mahony, and F.-X. Russotto, "Landing a vtol unmanned aerial vehicle on a moving platform using optical flow," *IEEE Transactions on Robotics*, vol. 28, no. 1, p. 77–89, 2012.

[22] D. Lee, T. Ryan, and H. J. Kim, "Autonomous landing of a vtol uav on a moving platform using image-based visual servoing," in *2012 IEEE International Conference on Robotics and Automation*, 2012, pp. 971–976.

[23] A. Tahir, "Autonomous swarming drones — landing a swarm of quadcopters on a vessel," Master's thesis, NOVIA University of Applied Sciences, Turku, Finland, December 2019.

[24] K. Kanjanawanishkul, "Formation control of mobile robots: Survey," *UBU Engineering Journal*, vol. 4, no. 1, p. 50–64, 2011.

[25] F. Šolc, "Modelling and control of a quadrocopter," *Advances in Military Technology*, vol. 5, no. 2, p. 29–38, 2010.

[26] P. Wang and F. Hadaegh, "Coordination and control of multiple microspacecraft moving in formation," *Journal of the Astronautical Sciences*, vol. 44, no. 3, p. 315–355, 1996.

[27] D. Galzi and Y. Shtessel, "Uav formations control using high order sliding modes," in *2006 American Control Conference*, 2006, p. 4249–4254.

[28] B. Yun, B. Chen, K. Lum, and T. Lee, "Design and implementation of a leader-follower cooperative control system for unmanned helicopters," *Journal of Control Theory and Applications*, vol. 8, no. 1, p. 61–68, 2010.

[29] M. Lewis and K. Tan, "High precision formation control of mobile robots using virtual structures," *Autonomous Robots*, vol. 4, no. 4, p. 387–403, 1997.

[30] T. Paul, T. Krogstad, and J. Gravdahl, "Modelling of uav formation flight using 3d potential field," *Simulation Modelling Practice and Theory*, vol. 16, no. 9, p. 1453–1462, 2008.

[31] Z. Chao, S. Zhou, L. Ming, and W. Zhang, "Uav formation flight based on nonlinear model predictive control," *Mathematical Problems in Engineering*, vol. 2012, p. 1–15, 2012.

[32] T. Balch and R. C. Arkin, "Behavior-based formation control for multirobot teams," *IEEE Transactions on Robotics and Automation*, vol. 14, no. 6, p. 926–939, 1998.

[33] J. R. T. Lawton, R. W. Beard, and B. J. Young, "A decentralized approach to formation maneuvers," *IEEE Transactions on Robotics and Automation*, vol. 19, no. 6, p. 933–941, 2003.

[34] D. Bennet and C. McInnes, "Verifiable control of a swarm of unmanned aerial vehicles," *Proceedings of the Institution of Mechanical Engineers, Part G: Journal of Aerospace Engineering*, vol. 223, no. 7, p. 939–953, 2009.

[35] K.-K. Oh, M.-C. Park, and H.-S. Ahn, "A survey of multi-agent formation control," *Automatica*, vol. 53, p. 424–440, 2015.

[36] A. Tahir, J. Böling, M.-H. Haghbayan, and J. Plosila, "Comparison of linear and nonlinear methods for distributed control of a hierarchical formation of uavs," *IEEE Access*, DOI: 10.1109/ACCESS.2020.2988773.